

~~CONFIDENTIAL~~

Copy 5
RM L52G11a

NACA RM L52G11a



SEP 19 1952

NACA

Lee

RESEARCH MEMORANDUM

WIND-TUNNEL INVESTIGATION OF THE STATIC LATERAL
STABILITY CHARACTERISTICS OF WING-FUSELAGE
COMBINATIONS AT HIGH SUBSONIC SPEEDS

SWEEP SERIES

By Richard E. Kuhn and Paul G. Fournier

Langley Aeronautical Laboratory
Langley Field, Va.

FOR REFERENCE

NOT TO BE TAKEN FROM THIS ROOM

CLASSIFIED DOCUMENT

This material contains information affecting the National Defense of the United States within the meaning of the espionage laws, Title 18, U.S.C., and the transmission or revelation of which in any manner to an unauthorized person is prohibited by law.

CLASSIFICATION CANCELLED

Authority: *Declass. Re. Act of 7-28-52*

RN-104

By: *ALB 8-13-56*

See

NATIONAL ADVISORY COMMITTEE FOR AERONAUTICS

WASHINGTON
September 9, 1952

~~CONFIDENTIAL~~

LIBRARY

NATIONAL ADVISORY COMMITTEE FOR AERONAUTICS

RESEARCH MEMORANDUM

WIND-TUNNEL INVESTIGATION OF THE STATIC LATERAL
STABILITY CHARACTERISTICS OF WING-FUSELAGE
COMBINATIONS AT HIGH SUBSONIC SPEEDS

SWEEP SERIES

By Richard E. Kuhn and Paul G. Fournier

SUMMARY

An investigation was made in the Langley high-speed 7- by 10-foot tunnel to determine the effect of sweep on the static lateral stability characteristics of wing-fuselage combinations having wings of aspect ratio 4 and taper ratio 0.6 at high subsonic speeds. The parameter $C_{l_{\beta}C_L}$, which expresses the rate of change of effective dihedral with

lift coefficient, increased in magnitude with increasing Mach number for all wings tested except the 60° swept wing. This result is in contrast to the slight reduction predicted by available theory. Above the force-break Mach number this parameter $C_{l_{\beta}C_L}$ exhibited a rapid decrease in

magnitude with Mach number. The fuselage accounted almost entirely for the measured values of the derivative of yawing moment due to sideslip $C_{n_{\beta}}$ and lateral force due to sideslip $C_{Y_{\beta}}$ at the lower lift coefficients. Mach number had little effect on the lateral stability characteristics of the fuselage alone.

INTRODUCTION

A systematic research program is being carried out in the Langley high-speed 7- by 10-foot wind tunnel to determine the aerodynamic characteristics of various arrangements of the component parts of research-type airplane models, including some complete model configurations. Data are being obtained on characteristics in pitch and sideslip and

during steady roll at Mach numbers from 0.40 to about 0.95. The Reynolds number range for the sting-supported models varies from 2×10^6 to 3.5×10^6 , depending on the wing plan form and the test Mach number.

This paper presents results which show the effect of sweep on the aerodynamic characteristics in sideslip of wings of aspect ratio 4, taper ratio 0.6, and with an NACA 65A006 airfoil section in combination with a fuselage that was common to all configurations. The pitch characteristics of these wing-fuselage combinations are presented in reference 1. The pitch data for the fuselage alone and for some of the related wing-fuselage configurations of this program are presented in reference 2. In order to expedite the issuance of the results, only a limited comparison of some of the more significant characteristics with available theory is presented.

COEFFICIENTS AND SYMBOLS

The stability system of axes used for the presentation of the data, together with an indication of the positive directions of forces, moments, and angles, are presented in figure 1. All moments are referred to the quarter-chord point of the mean aerodynamic chord.

C_L	lift coefficient, Lift/qS
C_l	rolling-moment coefficient, Rolling moment/qSb
C_n	yawing-moment coefficient, Yawing moment/qSb
C_y	lateral-force coefficient, Lateral force/qS
q	dynamic pressure, $\rho V^2/2$, lb/sq ft
ρ	mass density of air, slugs/cu ft
V	free-stream velocity, fps
M	Mach number
R	Reynolds number, $\frac{\rho V \bar{c}}{\mu}$
μ	absolute viscosity of air, slugs/ft-sec

S	wing area, sq ft
b	wing span, ft
c	wing chord, ft
\bar{c}	mean aerodynamic chord, $\frac{2}{S} \int_0^{b/2} c^2 dy$, ft
y	spanwise station, ft
α	angle of attack, deg
β	angle of sideslip, deg
Γ'	local dihedral angle, $\frac{\partial \delta}{\partial y}$, radians
Γ	equivalent constant dihedral angle, radians
δ	deflection, ft

$$C_{l\beta} = \frac{\partial C_l}{\partial \beta}, \text{ per deg}$$

$$C_{n\beta} = \frac{\partial C_n}{\partial \beta}, \text{ per deg}$$

$$C_{Y\beta} = \frac{\partial C_Y}{\partial \beta}, \text{ per deg}$$

$$C_{l\beta C_L} = \frac{\partial C_{l\beta}}{\partial C_L}$$

$C_{l\beta\Gamma}$ value of $C_{l\beta}$ for unit dihedral angle Γ

Subscript:

WF-F wing-fuselage values minus fuselage values

MODELS AND APPARATUS

The wing-fuselage combinations tested are shown in figure 2 and are the same wing-fuselage combinations used in reference 1. All wings had an NACA 65A006 airfoil section parallel to the fuselage center line and were attached to the fuselage in a midwing position. All wings were constructed of solid aluminum alloy except the 45° swept wing which was of composite construction, consisting of a steel core and bismuth-tin covering. The aluminum fuselage was common to all configurations; the ordinates are presented in reference 2.

The wings of this investigation represent only a part of the family of wings being studied in a more extensive program; therefore, the wing designation system described in reference 2 is being utilized. For example, the wing designated by 45-4-0.6-006 has the quarter-chord line swept back 45° , an aspect ratio of 4, and a taper ratio of 0.6. The number 006 refers to the section designation; in this case the design lift coefficient is zero and the thickness is 6 percent of the chord.

The models were tested on the sting-type support system shown in figures 3 and 4. With this support system the model can be remotely operated through a 28° angle range in the plane of the vertical strut. By utilization of couplings in the sting behind the model, the model can be rolled through 90° so that either angle of attack (fig. 3) or angle of sideslip (fig. 4) can be the remotely controlled variable. With the wings horizontal (fig. 3) the couplings can be used to support the model at angles of sideslip of approximately -4° and 4° , while the model is tested through the angle-of-attack range.

TESTS AND CORRECTIONS

The tests were made in the Langley high-speed 7- by 10-foot tunnel through a Mach number range from approximately 0.4 to 0.95. The size of the models used caused the tunnel to choke at corrected Mach numbers of from 0.94 to 0.96, depending on the wing being tested. The blocking corrections which were applied were determined by the velocity-ratio method of reference 3.

Two groups of tests were made. The first group, from which the bulk of the data was obtained, was run at angles of sideslip of -4° and 4° through an angle-of-attack range from -3° to 24° (fig. 3). In addition, tests were made at several selected angles of attack through a sideslip-angle range from 4° to -10° .

The jet-boundary corrections which were applied to angle of attack were determined from reference 4. The corrections to lateral force, yawing moment, and rolling moment were considered negligible. Tare values were determined, but were found to be negligible and therefore were not applied. The angle of attack and angle of sideslip have been corrected for the deflection of the sting-support system and balance under load.

Under the action of an aerodynamic lift load, the wings assumed a curved dihedral distribution. With the model at a sideslip angle this dihedral produced a rolling moment which added to the rolling moment of the rigid wing and increased with lift; accordingly, a means of correcting the data to the rigid-wing case was developed.

In an attempt to approximate the dihedral distribution that existed during the tests, an elliptical load distribution was simulated by applying static loads at four spanwise points along the quarter-chord line of each wing. The deflection of the wing at several spanwise points was measured by dial gages and the resulting aeroelastic dihedral curves are presented in figure 5. The distributions of the local dihedral angle Γ' were determined by measuring the slope of these curves at several spanwise stations. An equivalent dihedral angle then was evaluated for each wing by the following relation:

$$\frac{\Gamma}{qC_L} = \frac{\int_0^1 \frac{\Gamma'}{qC_L} \frac{y}{b/2} cd\left(\frac{y}{b/2}\right)}{\int_0^1 \frac{y}{b/2} cd\left(\frac{y}{b/2}\right)}$$

The correction factor $\Delta C_{l\beta C_L}$ (fig. 6) was calculated by the following expression

$$\Delta C_{l\beta C_L} = - C_{l\beta \Gamma} \frac{\Gamma}{qC_L} \frac{q}{57.3}$$

where $C_{l\beta \Gamma}$ was obtained from reference 5. The effect of compressibility on $C_{l\beta \Gamma}$ was determined; however, this effect on $\Delta C_{l\beta C_L}$ was considered negligible. The corrections to yawing moment and lateral force were considered negligible.

The Reynolds number variation with test Mach number is presented in figure 7 and is based on the wing mean aerodynamic chord of 0.765 foot.

RESULTS AND DISCUSSION

The basic data for the wing-fuselage configurations are presented in figures 8 to 11. These data have not been corrected for aeroelastic distortion. The bulk of the data was obtained from tests at angles of sideslip of -4° and 4° . The flagged symbols (figs. 8 to 12) were obtained from the tests in which the angle of sideslip was the variable.

The basic data for the fuselage alone are presented in figure 12. It will be noted that Mach number has little effect on the fuselage-alone parameters. A comparison of figures 8 to 11 and figure 12 indicates that the lateral-force parameter C_{Y_β} and the yawing-moment parameter C_{n_β} are produced almost entirely by the fuselage.

A sample of the data obtained through the sideslip-angle range is presented in figure 13. The nonlinearity shown can be attributed almost entirely to the fuselage. This nonlinearity can be seen in the fuselage-alone lift and pitching-moment data of reference 2.

Rolling-Moment Characteristics

A comparison of the variation of the effective-dihedral parameter C_{l_β} with lift coefficient for the wing-fuselage configurations is presented in figure 14. The wing-plus-wing-fuselage-interference data (fig. 15) for the same conditions, which were obtained by subtracting the fuselage-alone data of figure 12 from the data of figure 14, show the same trends as the wing-fuselage data. At low lift coefficients the rate of change of C_{l_β} with lift coefficient increases with increasing sweep at all Mach numbers. The maximum value of C_{l_β} for the unswept wing decreased in magnitude at a Mach number of 0.91 and the variation with lift coefficient became quite smooth and free from the violent breaks and gradients exhibited at a Mach number of 0.80. This is probably due to the absence of a true stall at Mach numbers above 0.90 as shown by the lift and pitching-moment data of reference 1. The breaks in the C_{l_β} curves for all wings are analogous with the breaks in the lift and pitching-moment data for these wings (refs. 1 and 2), indicating that these variations are probably the result of partial stalling.

The variation of the slope C_{l_β/C_L} at zero lift (with and without aeroelastic corrections applied) with Mach number is presented in

figure 16 and the variation with sweep is shown in figure 17. The theoretical values were computed according to the method of reference 6 and corrected for the effects of Mach number by the method of reference 7. Up to an angle of sweepback of 45° , the experimental data corrected for aeroelastic distortion indicate an increase in the magnitude of $C_{l\beta C_L}$

with increasing Mach number, up to the force break, which is contrary to the slight decrease predicted by theory. The predicted trend with Mach number is obtained experimentally only with the 60° swept wing.

For the wings on which a force break was reached, $C_{l\beta C_L}$ exhibits a rapid reduction in magnitude with Mach number above this force-break Mach number. The 60° swept wing, for which the force break could not be reached, showed a small increase in the magnitude of $C_{l\beta C_L}$ as the maximum test Mach number was approached.

The experimental variation of $C_{l\beta C_L}$ with sweep angle (fig. 17) at a Mach number of 0.4 is in good agreement with the low-speed experimental results of reference 8 (fig. 17). The agreement between experiment and theory is only fair in that the experimental values of $C_{l\beta C_L}$ generally are considerably larger in magnitude than the predicted values, particularly at the higher Mach numbers.

Lateral-Force and Yawing-Moment Characteristics

A comparison of the variation of the lateral-stability parameters $C_{n\beta}$ and $C_{Y\beta}$ with lift coefficient is presented in figures 18 and 19 for the wing-fuselage configurations. The wing-plus-wing-fuselage-interference data for the same conditions, which were obtained by subtracting the fuselage-alone data of figure 12 from the data of figures 18 and 19, are presented in figures 20 and 21. At the lower lift coefficients the fuselage contribution to $C_{n\beta}$ and $C_{Y\beta}$ (figs. 20 and 21) accounts for about the entire measured values.

The breaks in the curves at the higher lift coefficients occur at approximately the same lift coefficients as the breaks in the $C_{l\beta}$ curves and are probably due to partial stalling which changes the magnitude and orientation of the resultant force on the two wing semispans.

CONCLUSIONS

The results of the present investigation of the aerodynamic characteristics in sideslip at high subsonic speeds of wings having various sweep angles, aspect ratio 4, taper ratio 0.6, and having an NACA 65A006 airfoil section indicate the following conclusions:

1. The experimental values (corrected for aeroelastic distortion) of $C_{l\beta C_L}$, which express the rate of change of effective dihedral with lift coefficient, increased in magnitude with increasing Mach number for all wings tested except the 60° swept wing. This result is in contrast to that of available theory which invariably predicts slight reductions in the magnitude of $C_{l\beta C_L}$ with increasing Mach number. Above the force-break Mach number this parameter exhibited a rapid decrease in magnitude with increasing Mach number.
2. At the lower lift coefficients the experimentally determined values of $C_{n\beta}$, the derivative of yawing moment due to sideslip, and $C_{Y\beta}$, the lateral force due to sideslip, are almost entirely due to the fuselage for the models tested.
3. Mach number had little effect on the lateral stability characteristics of the fuselage alone.

Langley Aeronautical Laboratory
National Advisory Committee for Aeronautics
Langley Field, Va.

REFERENCES

- ✓ 1. Wiggins, James W., and Kuhn, Richard E.: Wind-Tunnel Investigation of the Aerodynamic Characteristics in Pitch of Wing-Fuselage Combinations at High-Subsonic Speeds. Sweep Series. NACA RM L52D18, 1952.
2. Kuhn, Richard E., and Wiggins, James W.: Wind-Tunnel Investigation of the Aerodynamic Characteristics in Pitch of Wing-Fuselage Combinations at High Subsonic Speeds. Aspect-Ratio Series. NACA RM L52A29, 1952.
3. Hensel, Rudolf W.: Rectangular-Wind-Tunnel Blocking Corrections Using the Velocity-Ratio Method. NACA TN 2372, 1951.
4. Gillis, Clarence L., Polhamus, Edward C., and Gray, Joseph L., Jr.: Charts for Determining Jet-Boundary Corrections for Complete Models in 7- by 10-Foot Closed Rectangular Wind Tunnels. NACA ARR L5G31, 1945.
5. Bird, John D.: Some Theoretical Low-Speed Span Loading Characteristics of Swept Wings in Roll and Sideslip. NACA Rep. 969, 1950. (Supercedes NACA TN 1839.)
6. Toll, Thomas A., and Queijo, M. J.: Approximate Relations and Charts for Low-Speed Derivatives of Swept Wings. NACA TN 1581, 1948.
7. Fisher, Lewis R.: Approximate Corrections for the Effects of Compressibility on the Subsonic Stability Derivatives of Swept Wings. NACA TN 1854, 1949.
8. Letko, William, and Wolhart, Walter D.: Effect of Sweepback on the Low-Speed Static and Rolling Stability Derivatives of Thin Tapered Wings of Aspect Ratio 4. NACA RM L9F14, 1949.

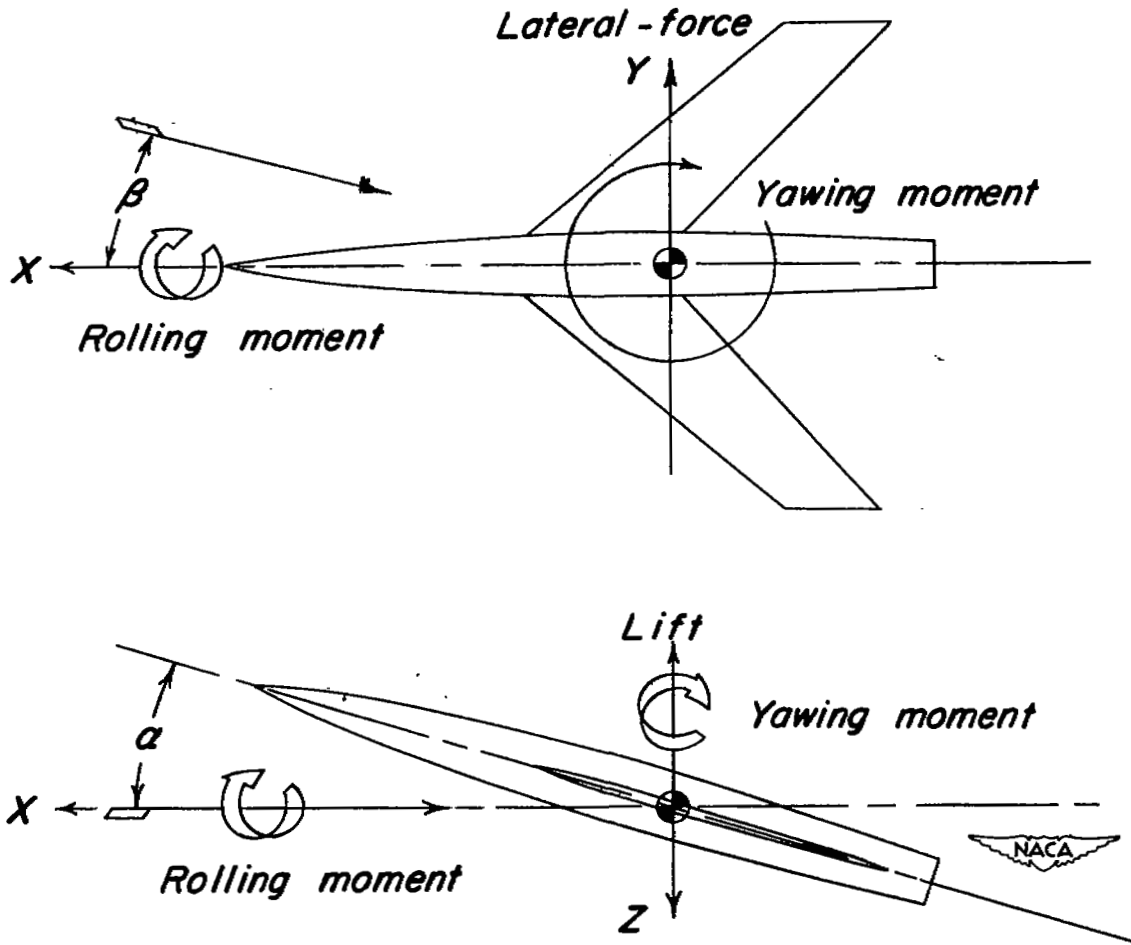


Figure 1.- System of axes used showing the positive direction of forces, moments, and angles.

Fuselage:
 Length 49.2 in.
 Max. diam. 5 in.
 Position of max. diam. 30 in.

0 10 20

 Scale, inches

Wing:
 Area 2.25 sqft
 Span 3.0ft
 Chord
 Tip 6.75 in.
 Root 11.25 in.
 Mean aerodynamic chord .765 ft
 Aspect ratio 4
 Taper ratio .6
 Incidence 0
 Dihedral 0
 Airfoil section
 parallel to fuselage @ NACA 65A006

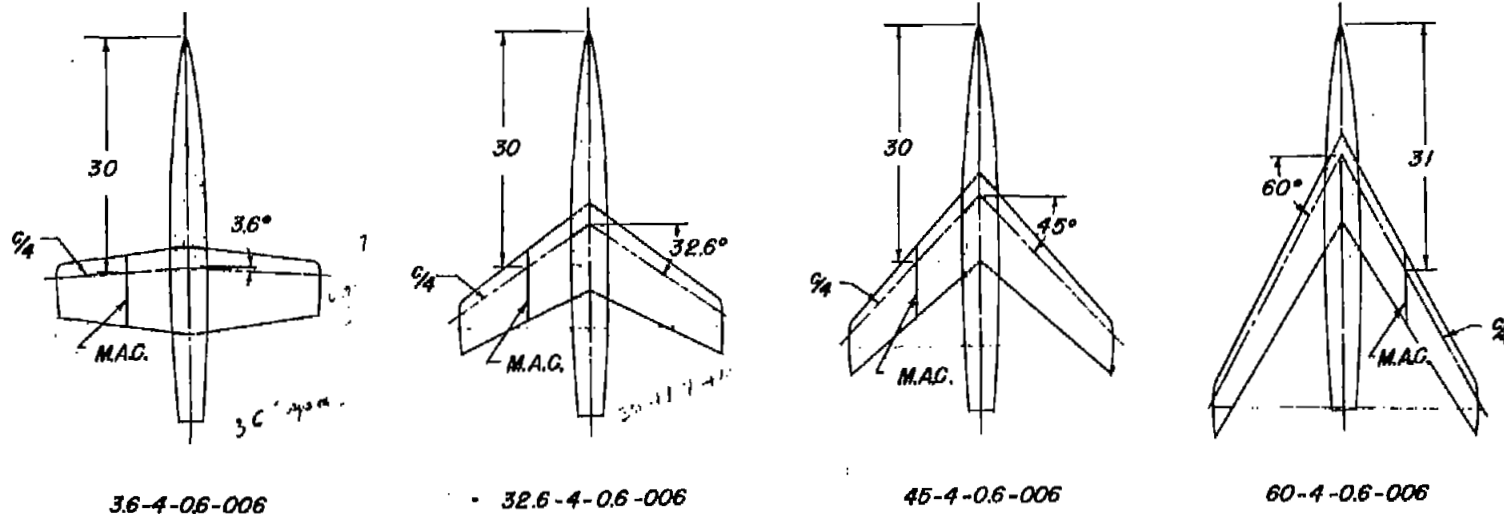


Figure 2.- Drawing of the four wing-fuselage configurations.



Figure 3.- A typical model installed on the sting support system for variable-angle-of-attack tests. Shown at 4° angle of sideslip.



Figure 4.- A typical model installed for variable-angle-of-sideslip tests. Shown at 0° angle of attack.

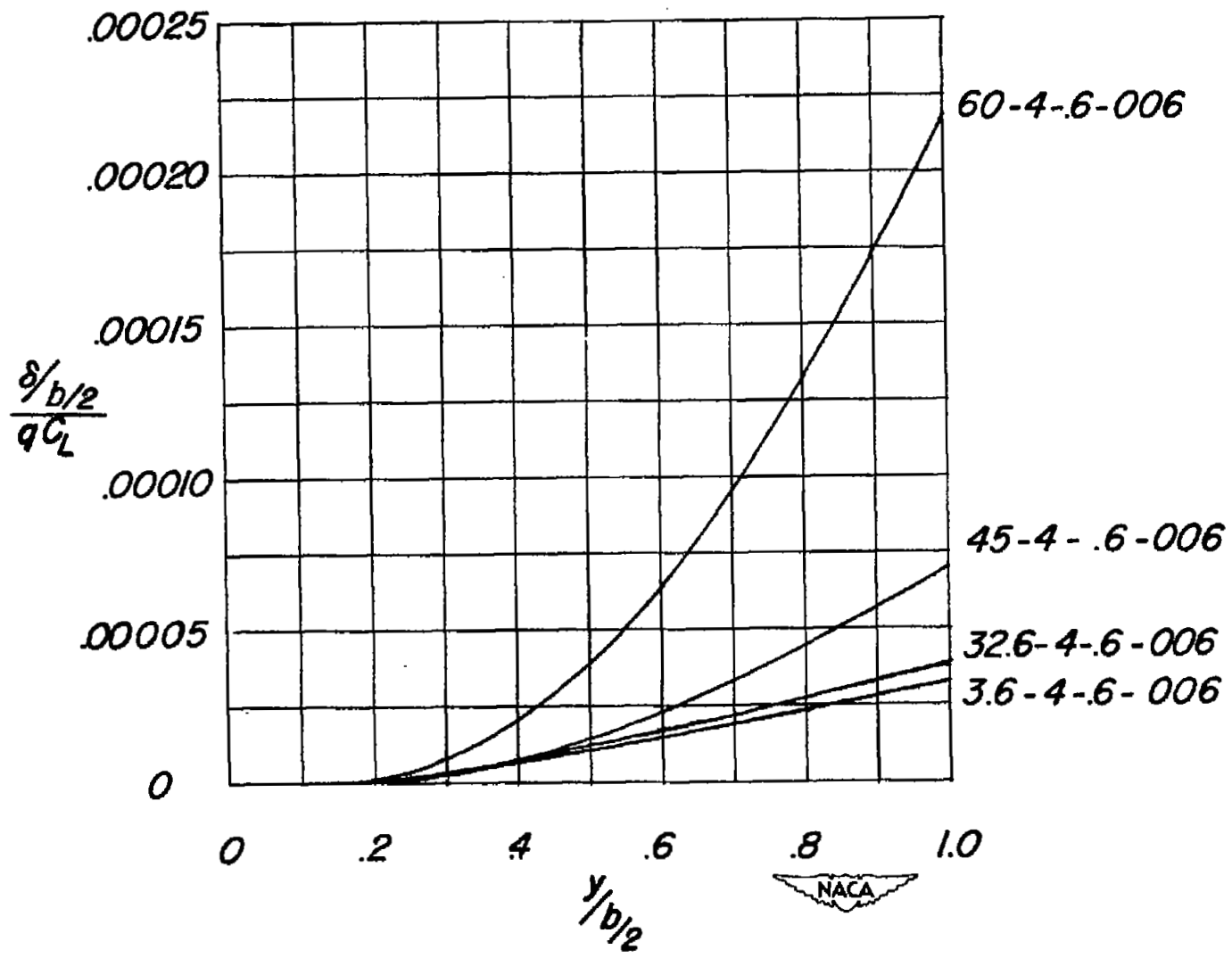


Figure 5.- Deflection curves for the test wing.

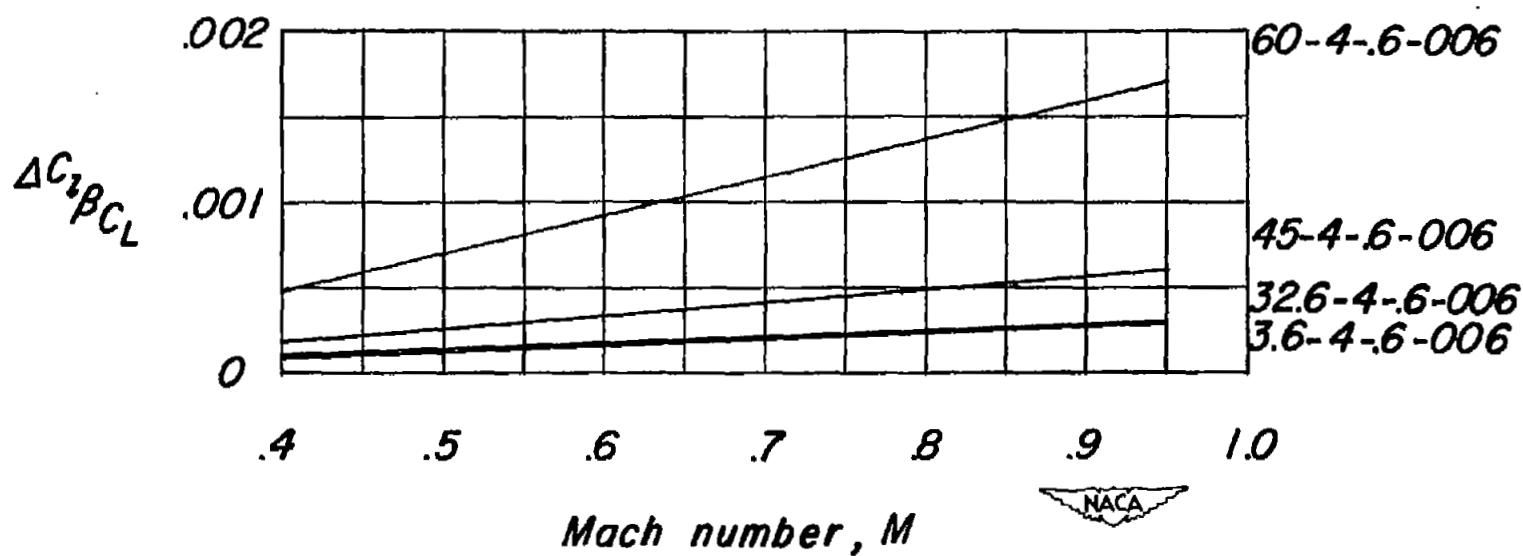


Figure 6.- Correction factors used to correct for the effects of aeroelastic distortion.

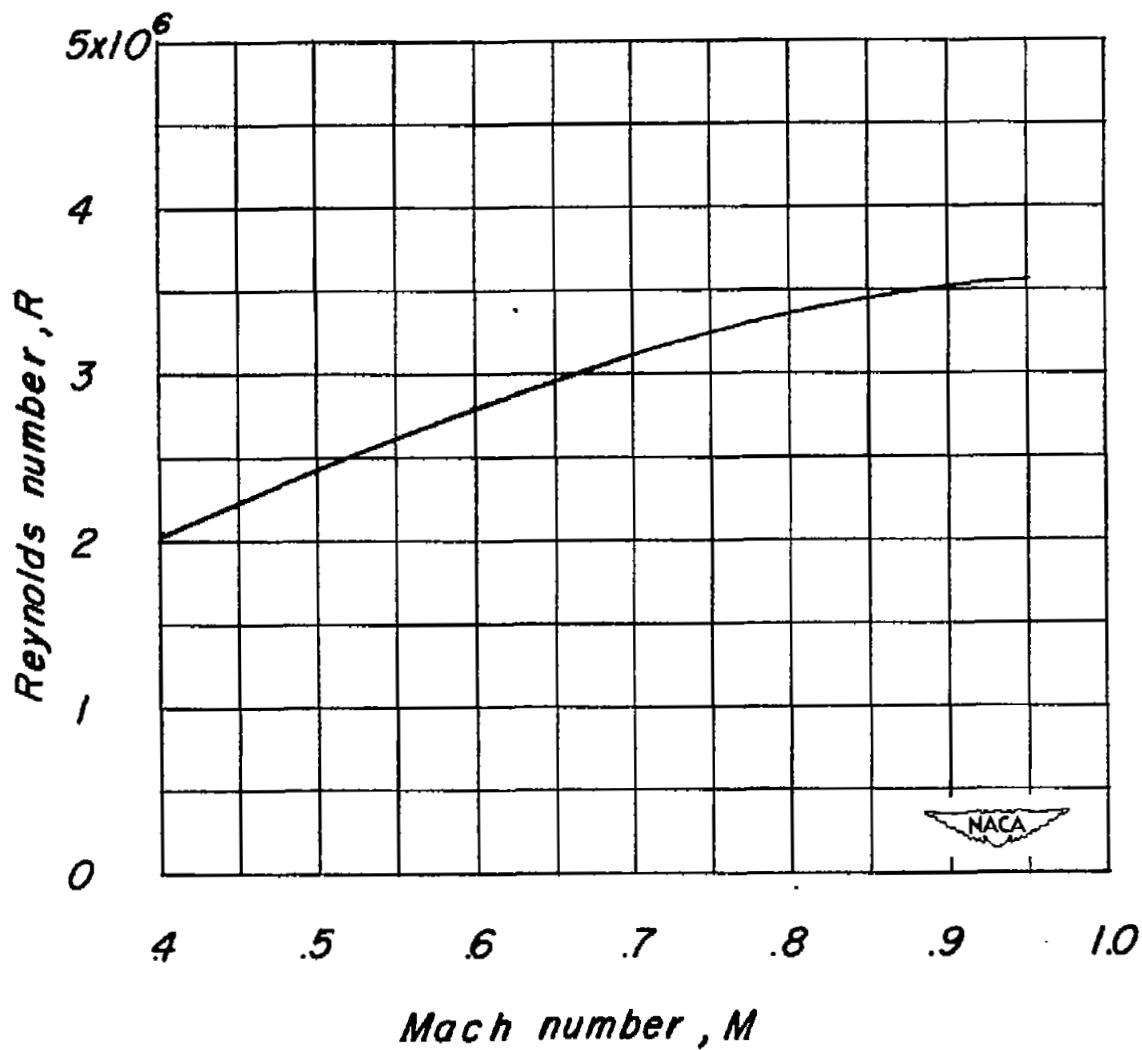


Figure 7.- Variation of mean Reynolds number with test Mach number based on the wing mean aerodynamic chord of 0.75 foot.

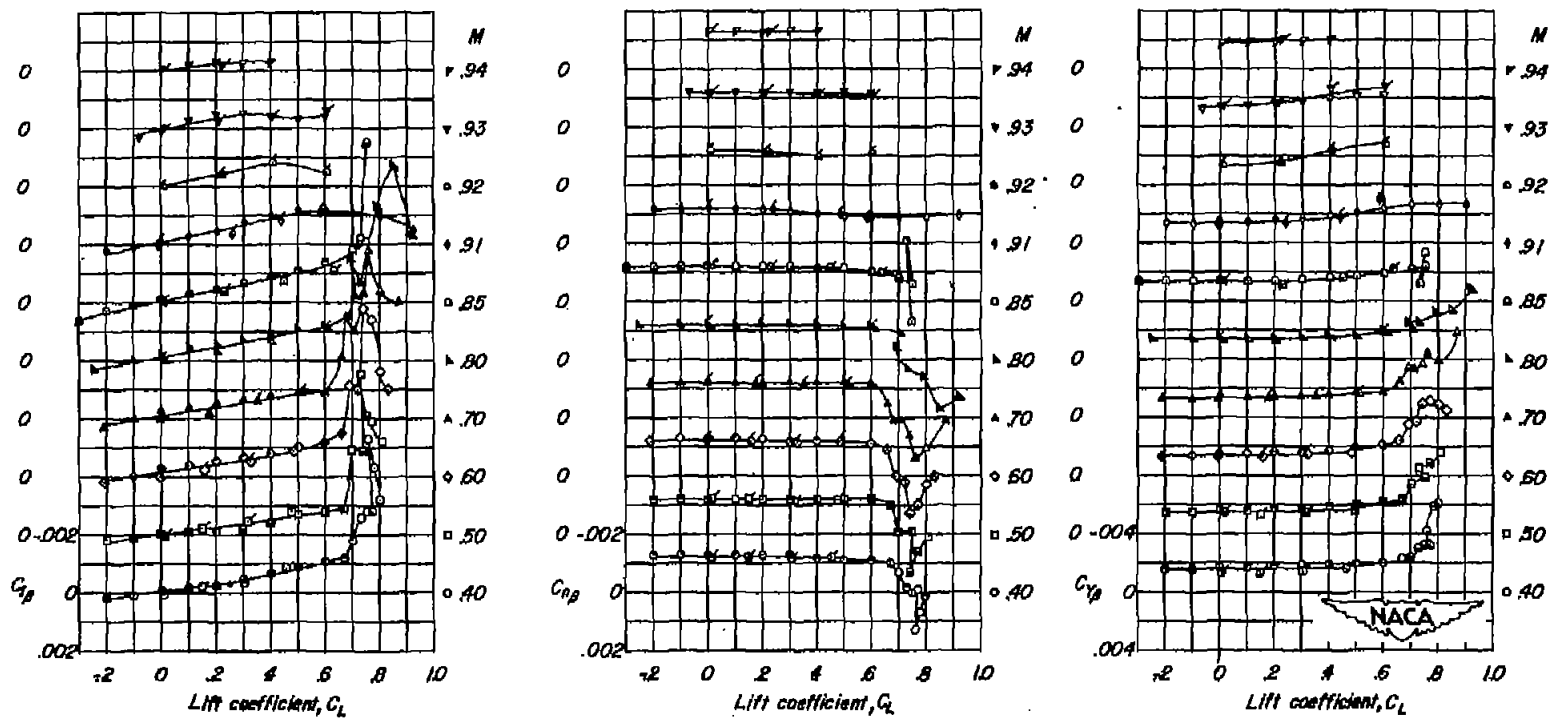


Figure 8.- Lateral stability characteristics of the 3.6-4-0.6-006 wing-fuselage combination. Not corrected for aeroelastic distortion. Flagged symbols represent tests in which the angle of sideslip was varied.

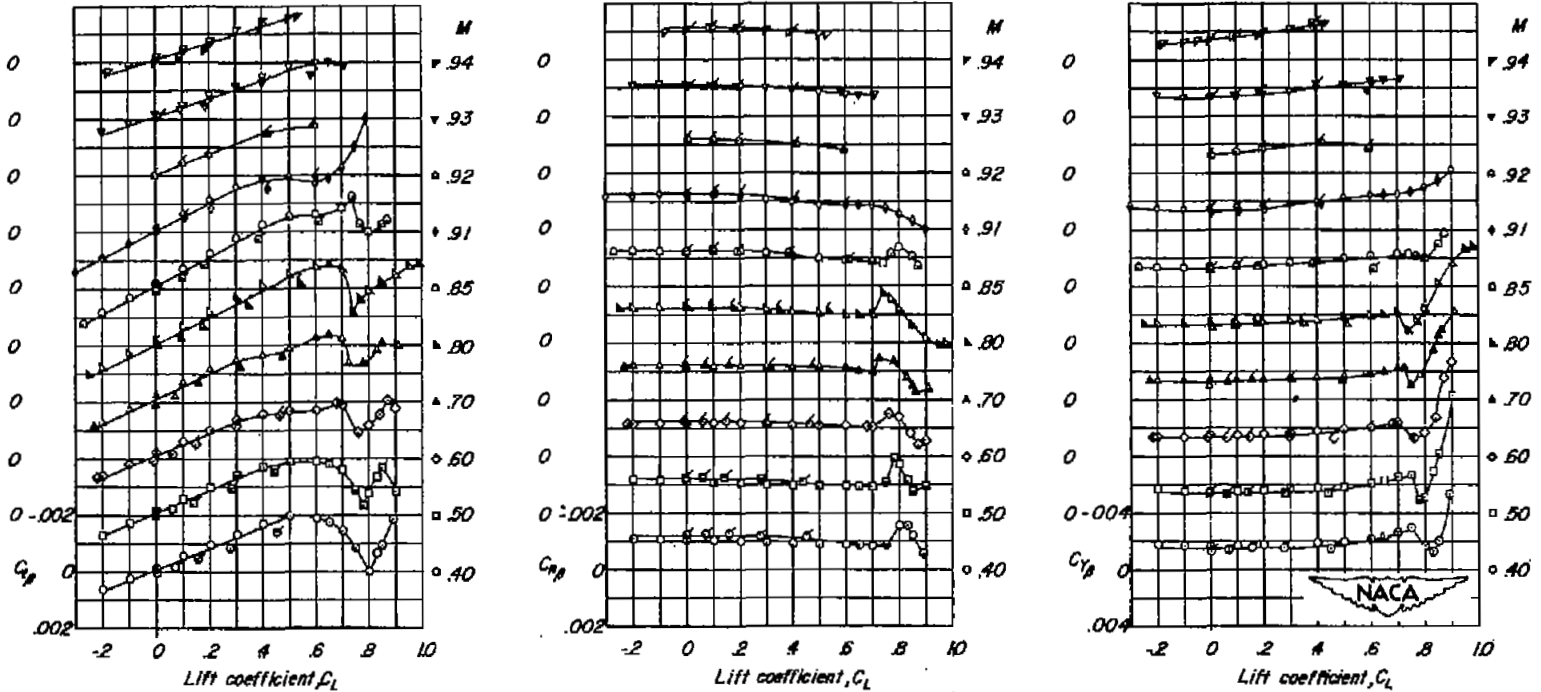


Figure 9.- Lateral stability characteristics of the 32.6-4-0.6-006 wing-fuselage configuration. Not corrected for aeroelastic distortion. Flagged symbols represent tests in which the angle of sideslip was varied.

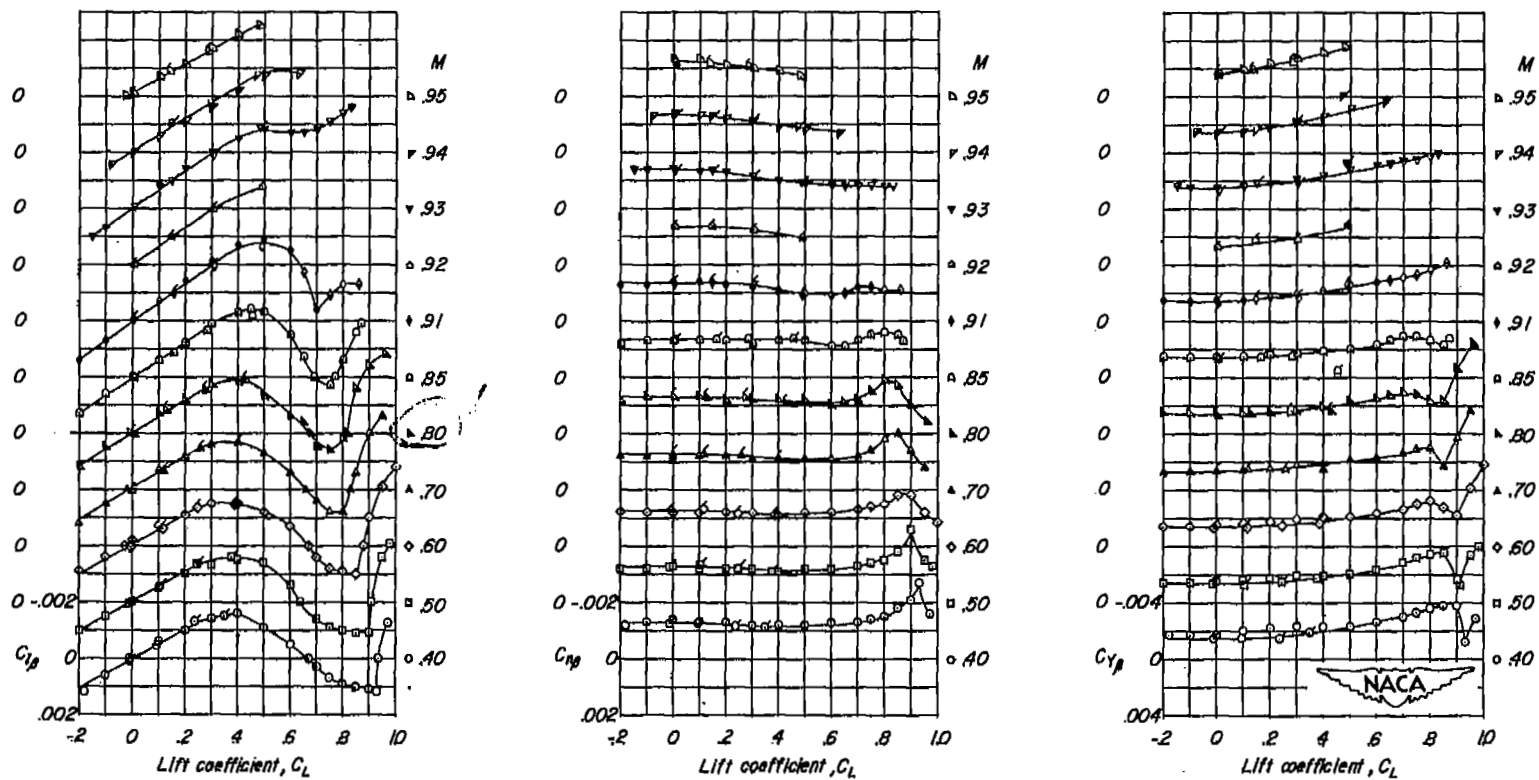


Figure 10.- Lateral stability characteristics of the 45-4-0.6-006 wing-fuselage configuration. Not corrected for aeroelastic distortion. Flagged symbols represent tests in which the angle of sideslip was varied.

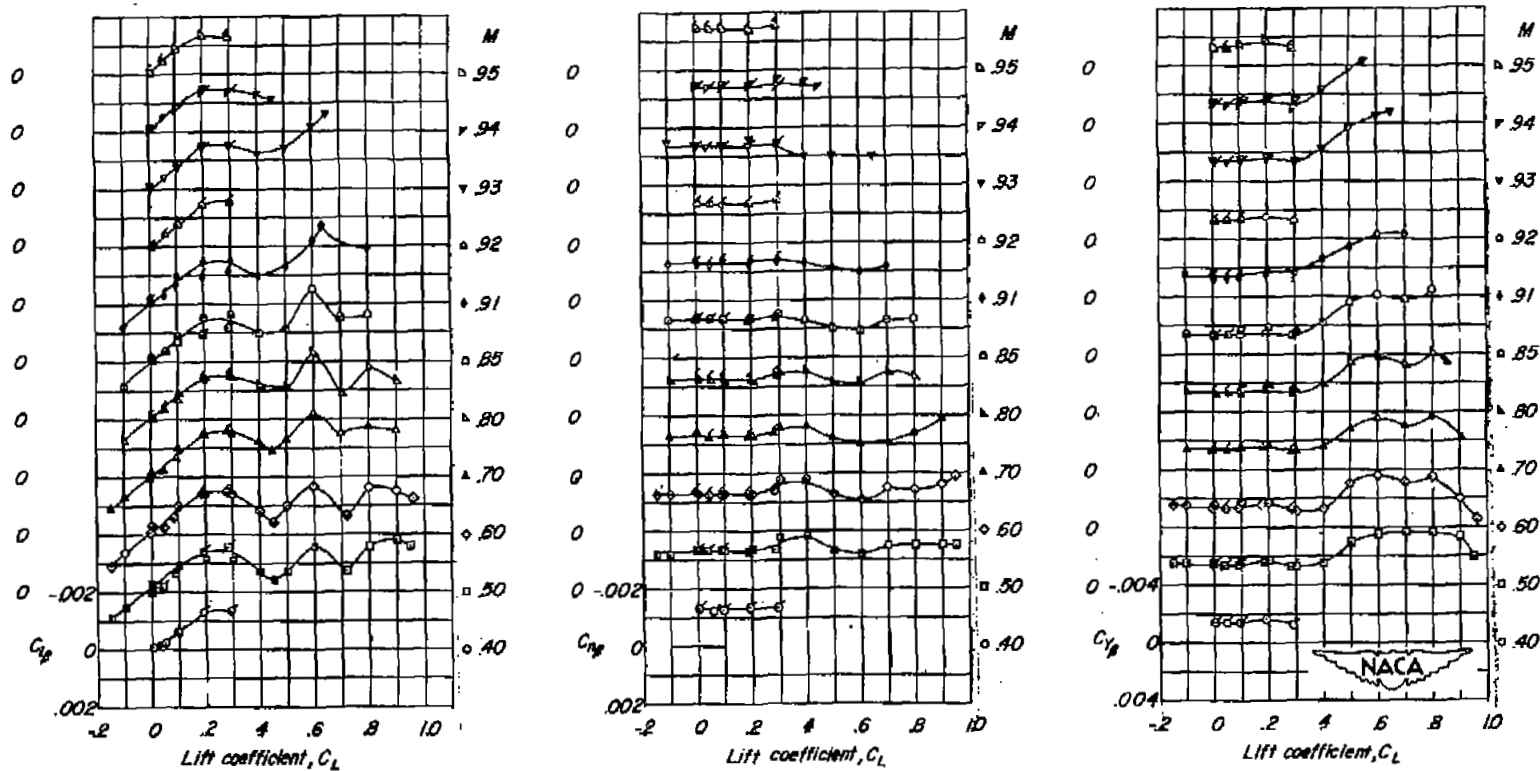


Figure 11.- Lateral stability characteristics of the 60-4-0.6-006 wing-fuselage configuration. Not corrected for aeroelastic distortion. Flagged symbols represent tests in which the angle of sideslip was varied.

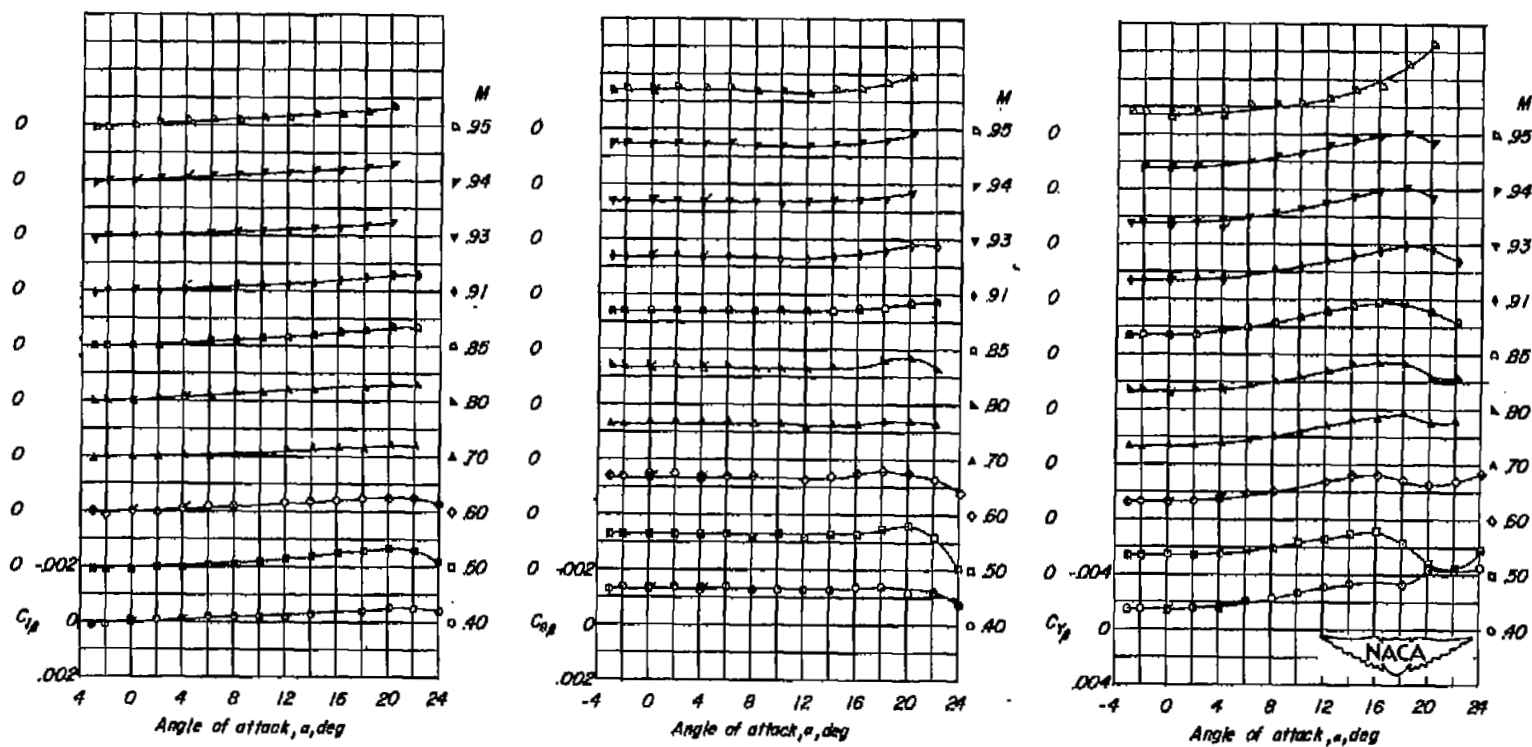


Figure 12.- Lateral stability characteristics of the fuselage alone. Flagged symbols represent tests in which the angle of sideslip was varied.

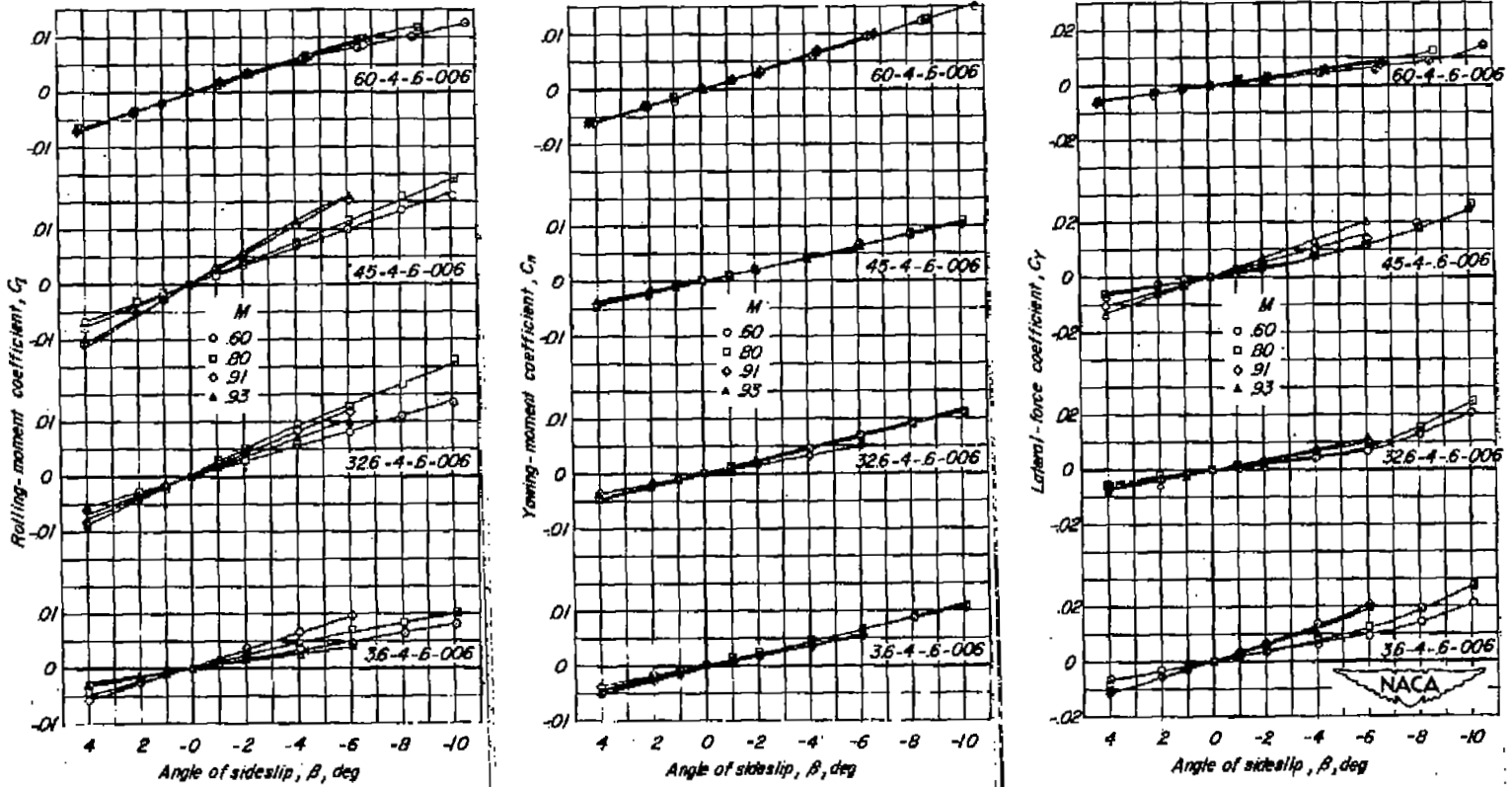


Figure 13.- Variation of the lateral coefficients with angle of sideslip at an angle of attack of about 6° .

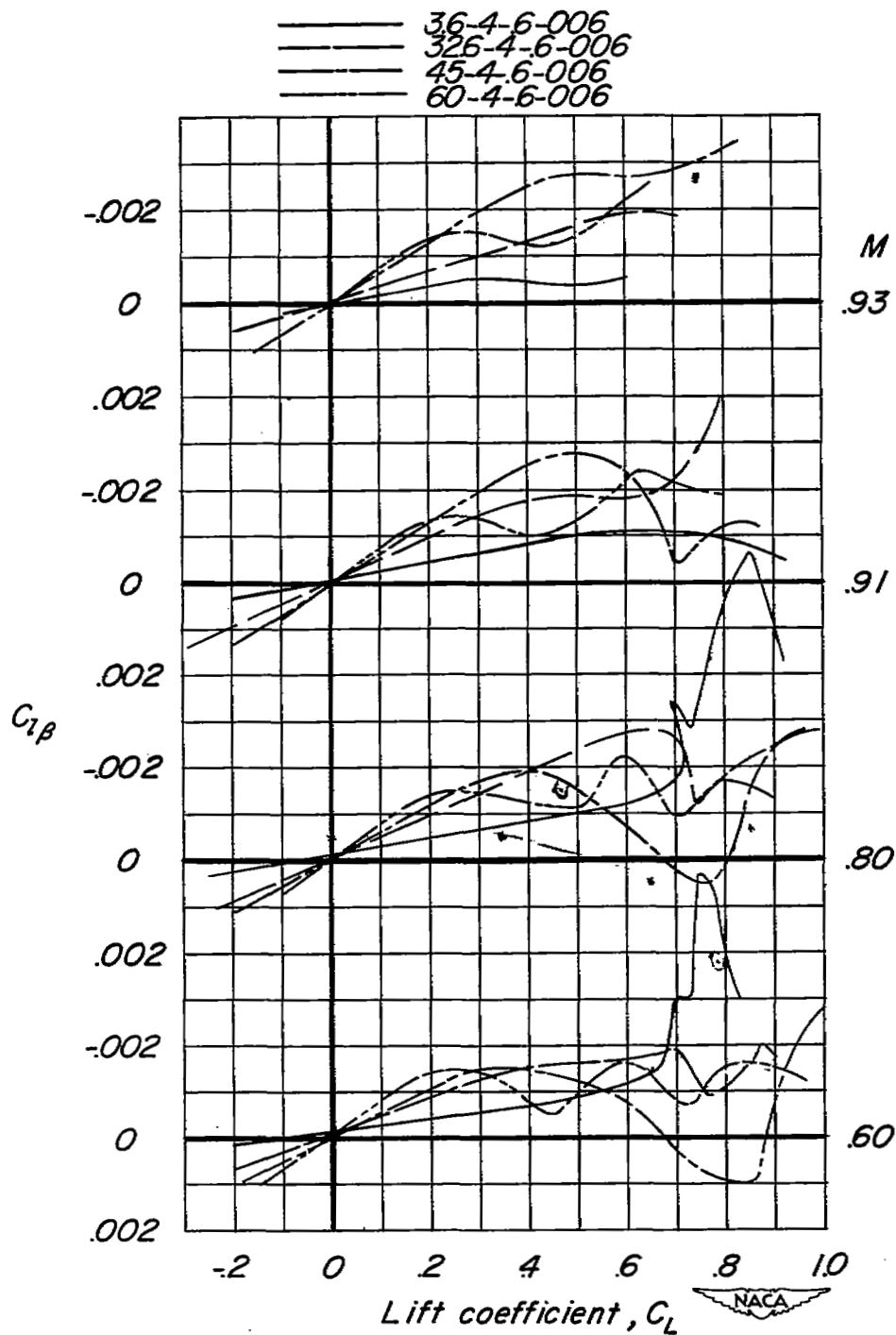


Figure 14.- Comparison of the variation of $C_{l\beta}$ with lift coefficient for the wing-fuselage configurations at several Mach numbers. Not corrected for aeroelastic distortion.

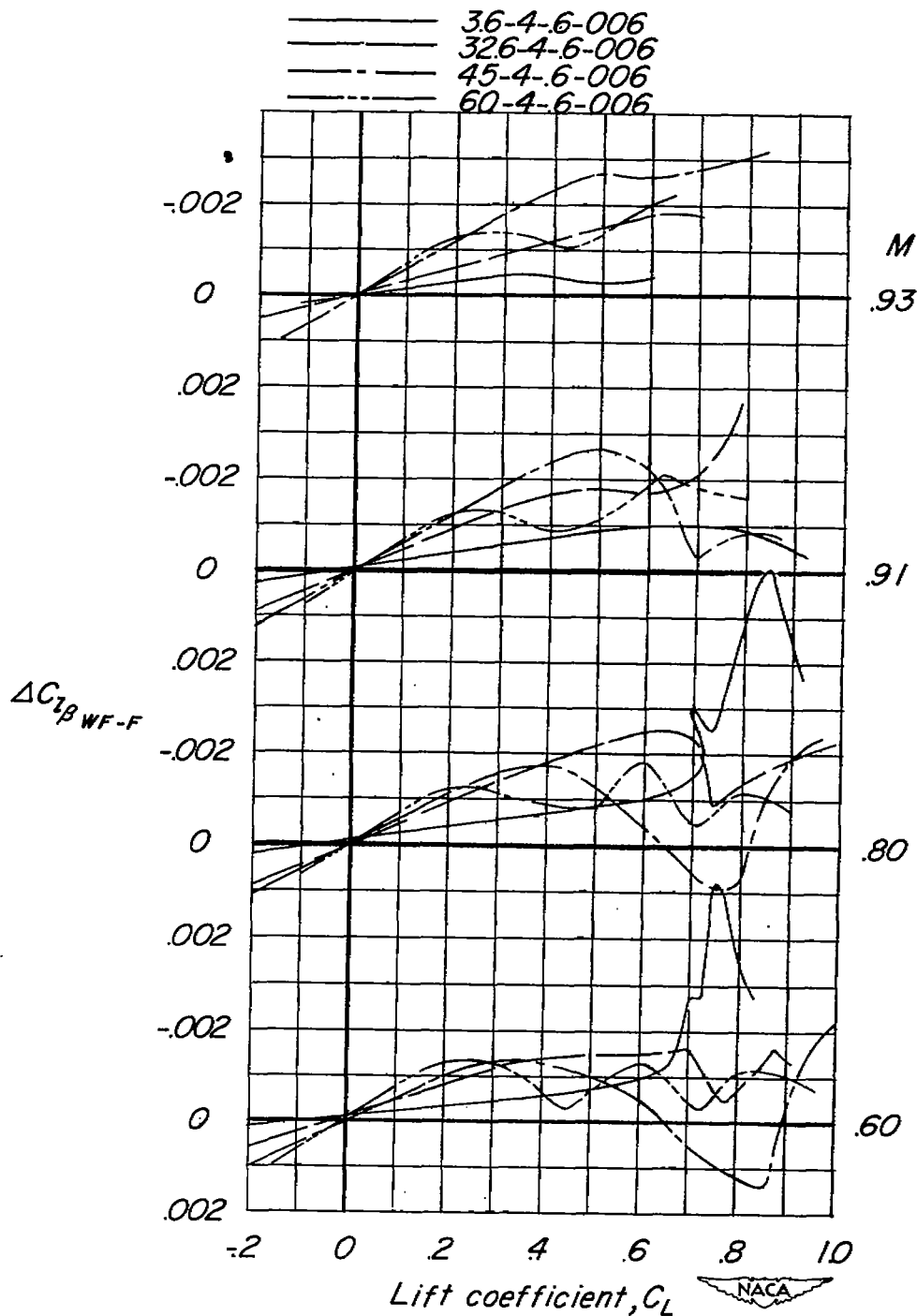


Figure 15.- Wing-plus-wing-fuselage-interference values of $C_{l_{\beta}}$ for the test wings compared at several Mach numbers. Not corrected for aeroelastic distortion.

—○— Measured values
 - - - Corrected for aeroelastic distortion
 — Theory, wing alone (Ref. 6 and 7)

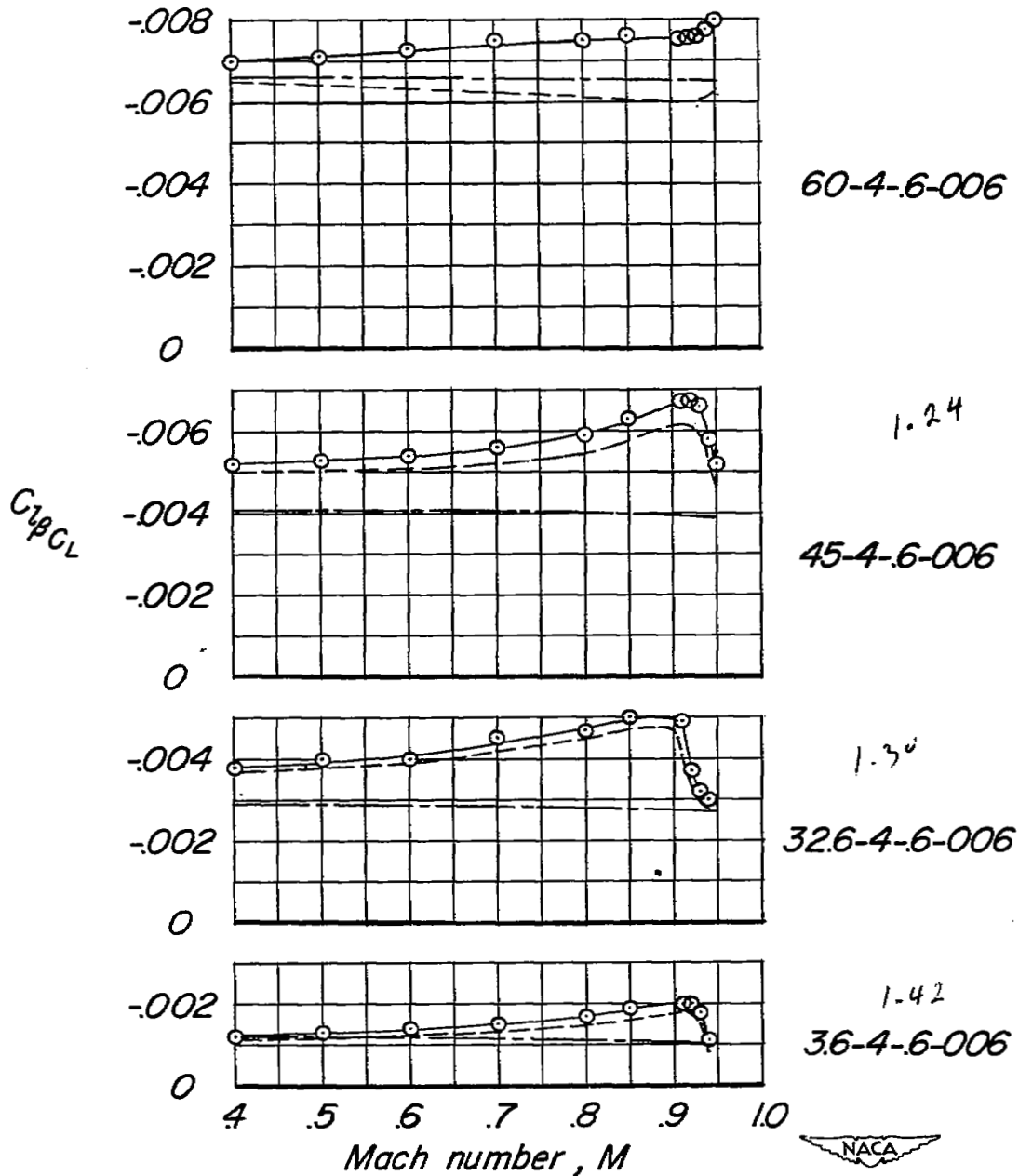


Figure 16.- Variation of $C_{l\beta C_L}$ with Mach number.

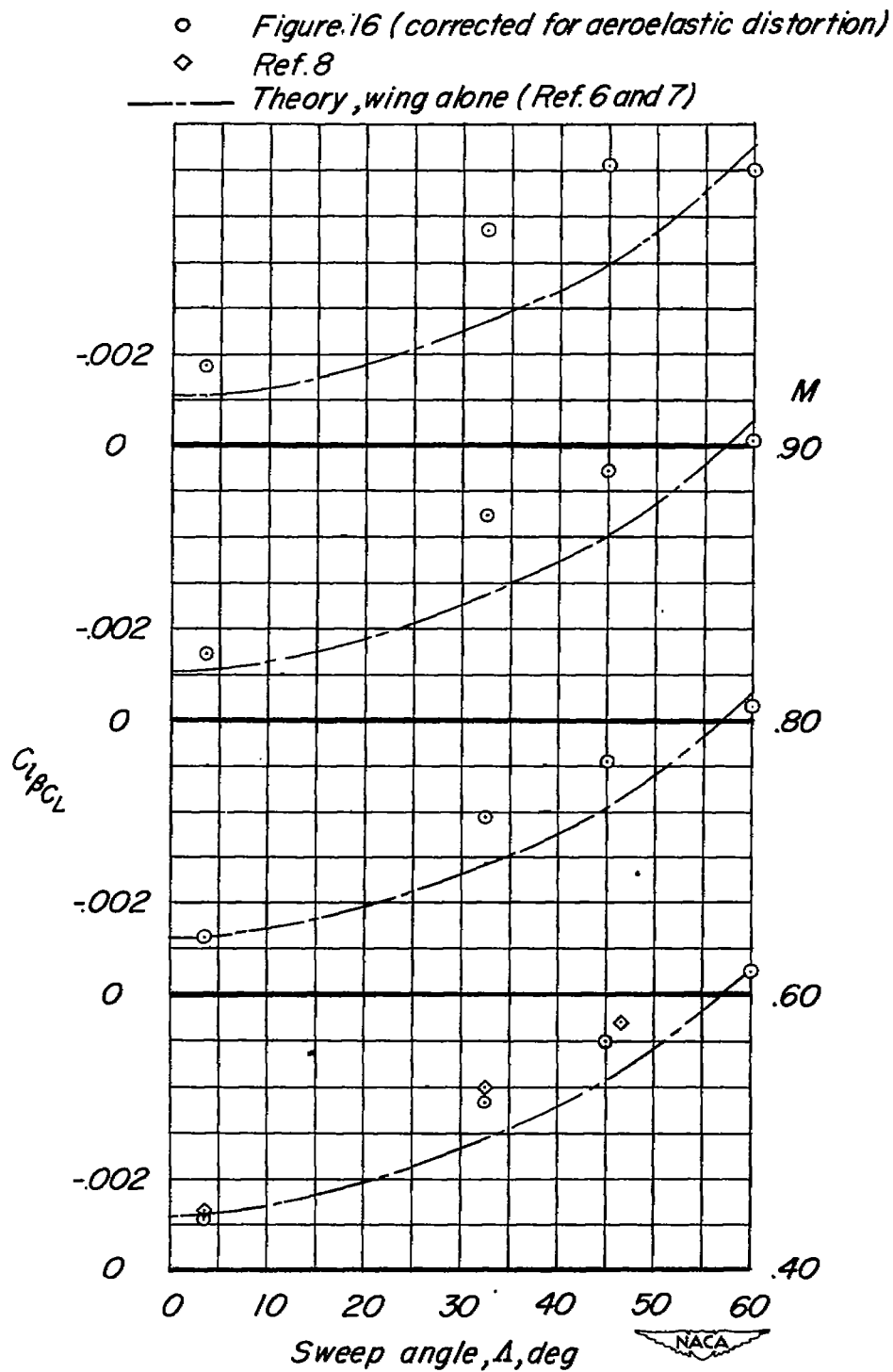


Figure 17.- Variation of $C_{l_{BC_L}}$ with sweep angle.

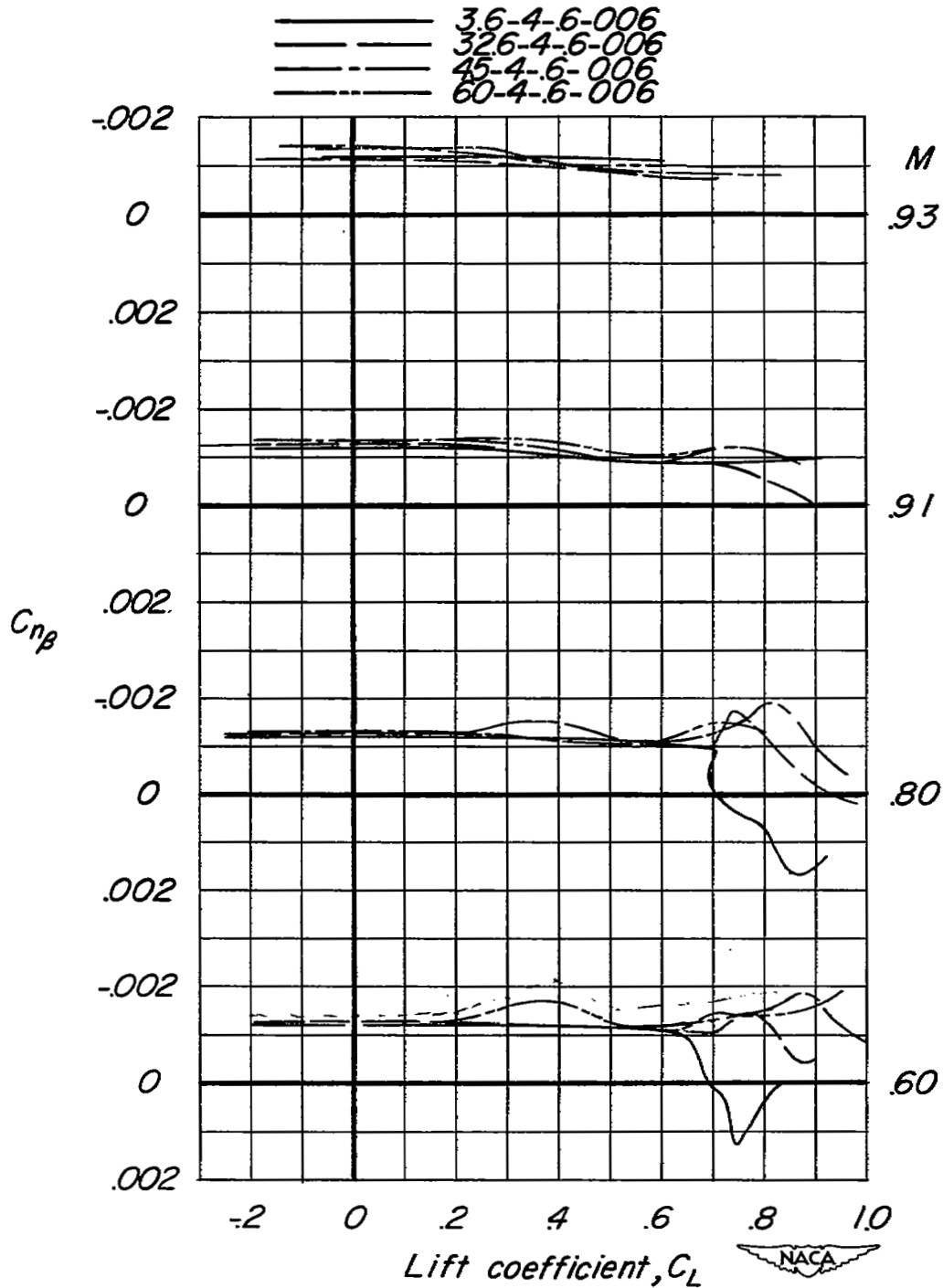


Figure 18.- Comparison of the variation of $C_{\eta\beta}$ for the wing-fuselage configuration with lift coefficient at several Mach numbers.

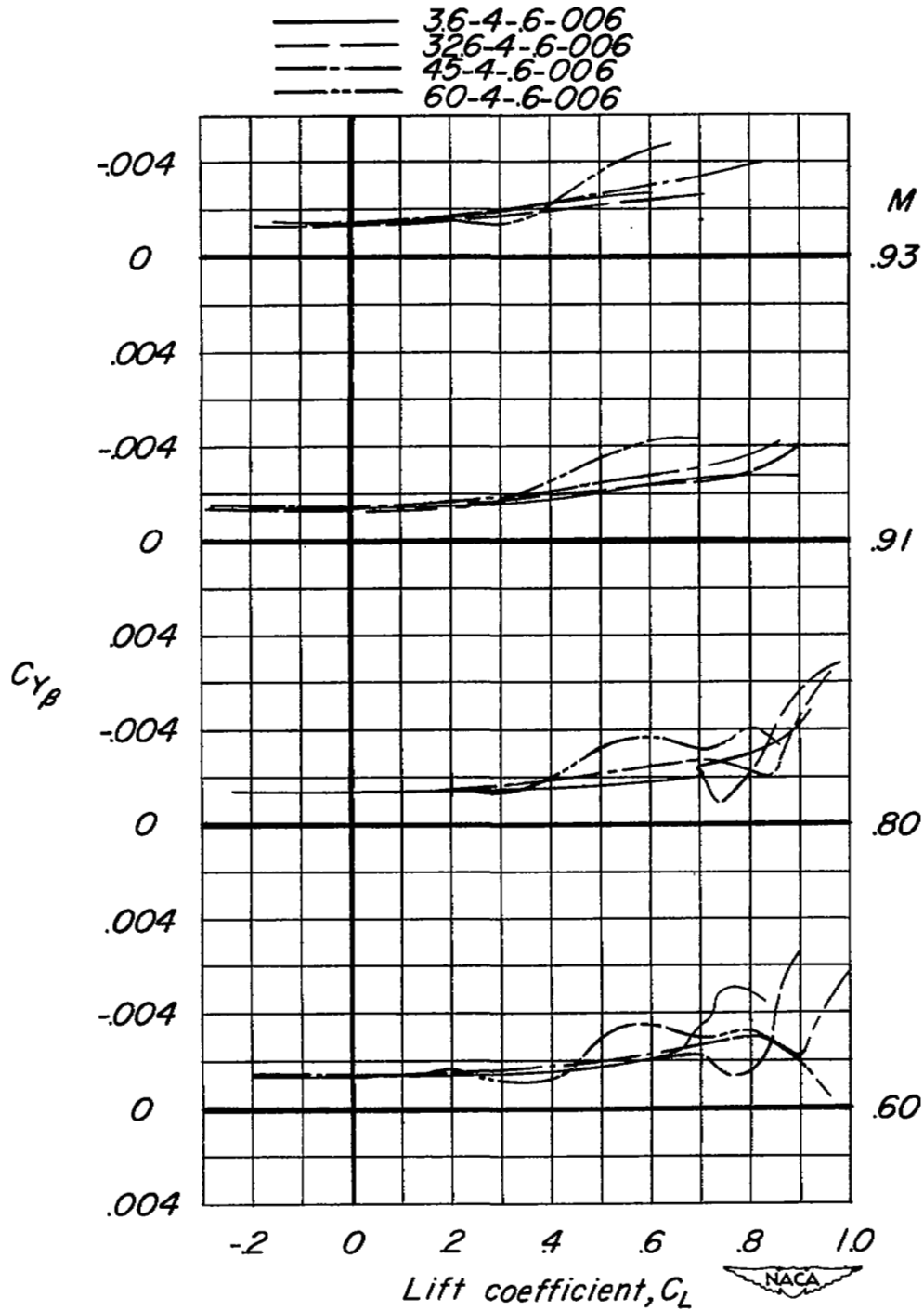


Figure 19.- Comparison of the variation of $C_{Y\beta}$ for the wing-fuselage configuration with lift coefficient at several Mach numbers.

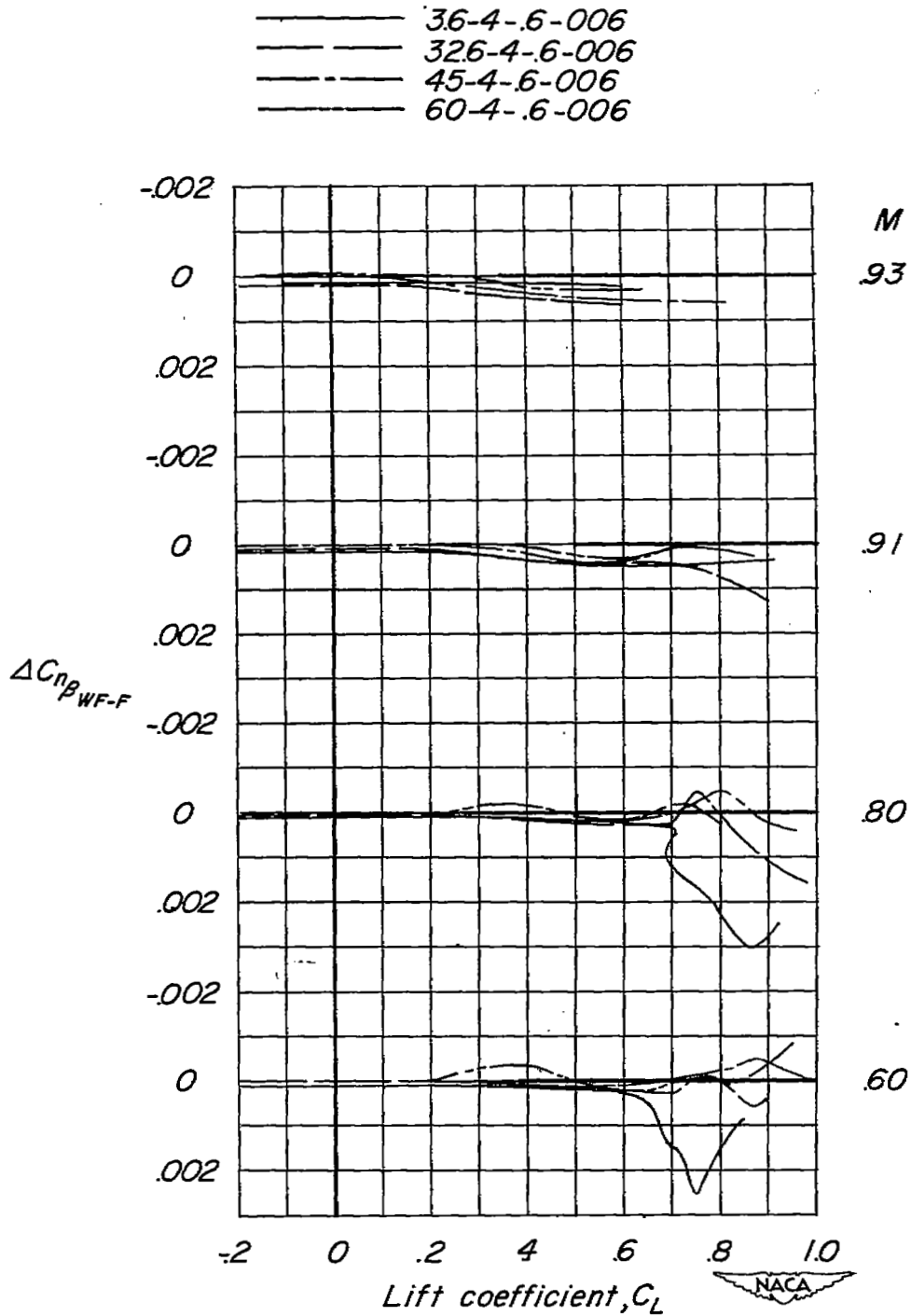


Figure 20.- Wing-plus-wing-fuselage-interference values of $C_{\eta\beta}$ for the test wings compared at several Mach numbers.

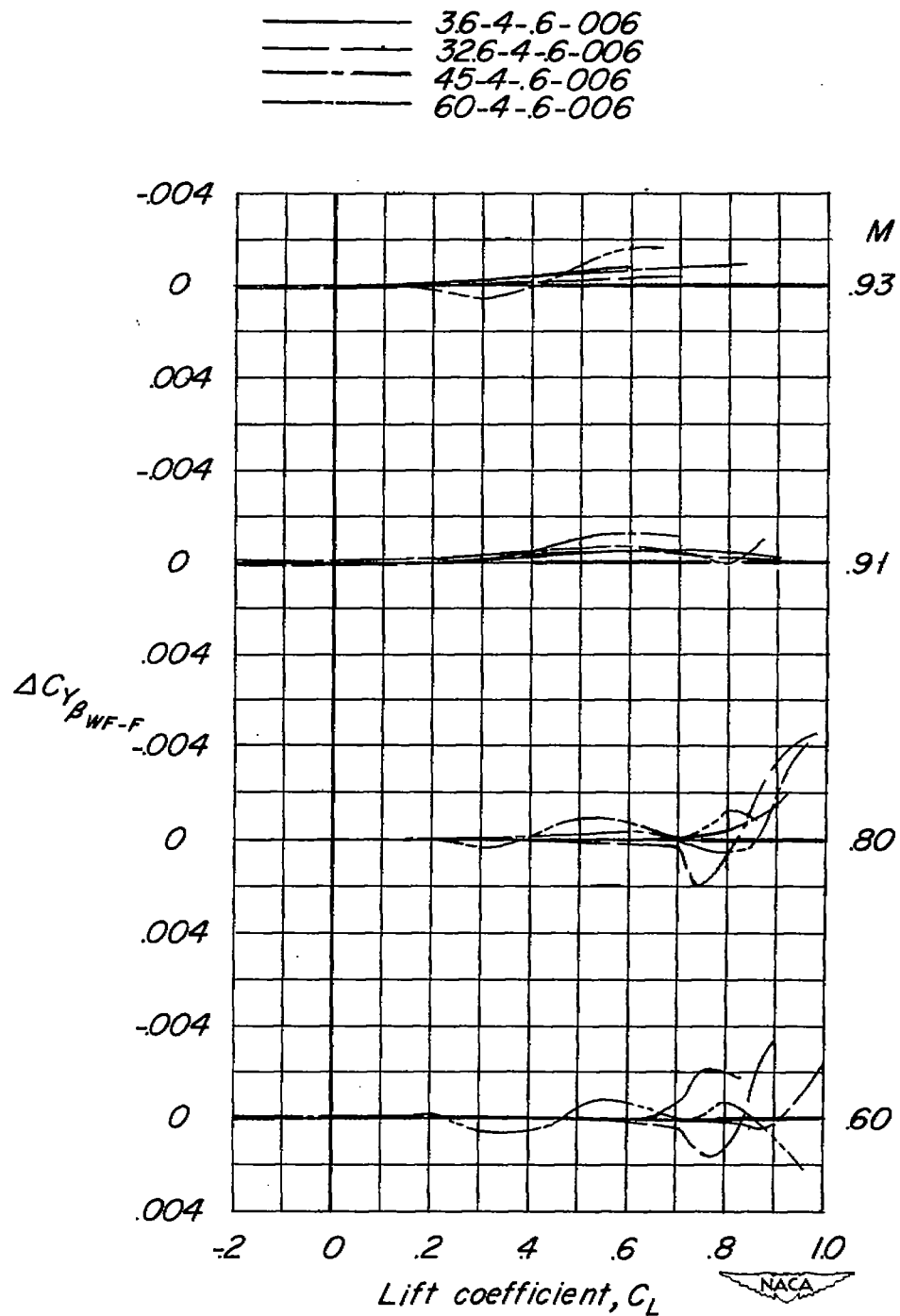


Figure 21.- Wing-plus-wing-fuselage-interference values of $C_{y_{\beta}}$ for the test wing compared at several Mach numbers.